

1
2
3
4 **SIMULATION-BASED NON-DESTRUCTIVE INSPECTION SCHEDULING OF**
5 **STEEL BRIDGES**
6

7
8 by

9
10
11 **Hsin-Yang Chung, Ph.D.**

12 Assistant Professor
13 Department of Civil Engineering
14 National Cheng-Kung University
15 No. 1 Ta-Hsueh Road
16 Tainan City 701, Taiwan
17 E-mail: hychung@mail.ncku.edu.tw
18 Tel: (886) 6-275-7575
19 Fax: (886) 6-235-8542

20
21 **Lance Manuel, Ph.D., P.E.**

22 Assistant Professor & Corresponding Author
23 Department of Civil Engineering
24 The University of Texas at Austin
25 Austin, TX 78712
26 E-mail: lmanuel@mail.utexas.edu
27 Tel: (512) 232-5691
28 Fax: (512) 471-7259

29
30 **Karl H. Frank, Ph.D., P.E.**

31 Professor
32 Department of Civil Engineering
33 The University of Texas at Austin
34 Austin, TX 78712
35 E-mail: kfrank@uts.cc.utexas.edu
36 Tel: (512) 471-4590
37 Fax: (512) 471-7259

38
39
40 Word count: 5242 + (1 table and 8 figures)

41 Submitted for:
42 Presentation at the 85th Annual Meeting of the Transportation Research Board
43 and
44 Publication in the Transportation Research Record Series.
45
46
47
48
49
50
51
52

ABSTRACT

A procedure for selecting an optimal NDI (non-destructive inspection) technique and associated schedule for fracture-critical member inspections on a specific steel bridge is presented. Information related to the probability of detection (POD) function (a measure of inspection quality) of alternative NDI techniques is utilized. Calculations based on use of the POD function together with Monte Carlo simulations of crack propagation in the detail of interest are performed. A cost function is formulated that includes inspection costs as well as possible failure costs with each candidate NDI technique and alternative inspection schedule. The selection of an NDI technique together with an associated schedule for fracture-critical inspections is thus formulated as an optimization problem that can guarantee minimum total cost. An optimal inspection frequency is sought as part of the optimization which utilizes appropriate constraints on inspection intervals and a minimum acceptable (target) structural safety level. A case study involving a box girder bridge is presented to illustrate the proposed probabilistic method.

Keywords: Probability of detection; Non-destructive inspection; Monte Carlo simulation.

INTRODUCTION

Many steel bridges are vulnerable to fatigue deterioration because of repetitive traffic loading cycles that they experience. The various non-destructive inspection (NDI) techniques suggested for use on steel bridges in the FHWA Bridge Inspector's Training Manual (Hartle et al. (1995)) include Ultrasonic Inspection (UI), Magnetic Particle Inspection (MI), Penetrant Inspection (PI), Radiographic Inspection (RI), Acoustic Emission Inspection (AEI), and Visual Inspection (VI). Inspection accuracy, accessibility, frequency, cost, and consequences of detection failures (misses) or false indications (false calls) must all be considered when selecting an NDI technique. Though other reliability-based fatigue inspection scheduling methods include consideration for inspection quality, such as those proposed for the offshore industry by Sorensen et al. (1991) and Cramer and Friis-Hansen (1992), it is not practical to calibrate inspection quality coefficients and other parameters in their models. Also, these methods often demand complicated reliability algorithms or extensive simulation schemes to obtain optimal inspection results; this limits their applicability to bridge maintenance with associated tighter budgetary constraints.

A probabilistic approach for dealing with inspection quality is proposed here for selection of the most economical NDI method. The approach involves Monte Carlo simulations and can help to select an NDI technique and accompanying schedule for inspection of fracture-critical members in a steel bridge. It also guarantees a specified acceptable safety level through the planned service life of the bridge. Available probability of detection (POD) functions associated with the various NDI techniques are employed as a measure of reliability. By combining calculations based on the POD functions together with Monte Carlo simulations of the crack growth for the fracture-critical member, a cost function is formulated that includes the expected cost of inspections and failure that result with each alternative NDI technique and inspection schedule. With appropriate constraints on inspection intervals and on a minimum (target) safety level, an optimal combination of NDI technique and inspection schedule that yields the minimum total cost can thus be obtained.

PROBABILITY OF DETECTION

The four possible outcomes of any NDI procedure are True Positive (hit), False Negative (miss), False Positive (false call), and True Negative (correct accept). The probability of detection (*POD*) of a crack of a given size is the conditional probability of a true positive call given that a crack with that size exists. An estimate of the *POD* can be obtained as:

$$\hat{POD} = \frac{N_{TP}}{N_{TP} + N_{FN}} \quad (1)$$

where \hat{POD} is the *POD* estimate for a specific crack size; N_{TP} is the number of true positive calls; and N_{FN} is the number of false negative calls. The false call probability (*FCP*) can also be evaluated as:

$$\hat{FCP} = \frac{N_{FP}}{N_{FP} + N_{TN}} \quad (2)$$

where \hat{FCP} is the *FCP* estimate for a specific crack size; N_{FP} is the number of false positive calls; and N_{TN} is the number of true negative calls.

By introducing cracks of various sizes into test specimens and performing inspections, *POD* estimates for various crack sizes and different NDI techniques can be obtained. Generally, two

analysis approaches – the Hit/Miss method and the Signal Response method – are employed to formulate the POD function, $POD(a)$, for any crack size, a , with any NDI technique.

Hit/Miss Method

This method is applied when inspection data are recorded in terms of hits or misses (i.e., indications of whether or not a crack is detected). This is commonly used for data from penetrant and visual inspection tests. The basic idea is to estimate the probability of detection, \hat{POD} , for any given crack size from the hit and miss data by applying regression analysis or a maximum likelihood procedure. Berens and Hovey (1981) proposed a log-logistic POD function based on hit/miss inspection data.

Signal Response Method

This method is applied for inspection results recorded in terms of the parameter \hat{a} that indicates signal response to stimuli (cracks), such as the inspection results produced by ultrasonic inspection and eddy current inspection. For \hat{a} values below the recording signal threshold, \hat{a}_{th} , no signal is recorded. Also, \hat{a} values are displayed when they are greater than a specified decisive value, \hat{a}_{dec} ; however, for crack sizes that exceed the signal saturation limit, \hat{a}_{sat} , of the recording system, the corresponding \hat{a} values stay the same as \hat{a}_{sat} . Between \hat{a}_{th} and \hat{a}_{sat} , \hat{a} values can be related to the true crack size, a , as follows:

$$\ln \hat{a} = \beta_0 + \beta_1 \ln a + \varepsilon; \quad \hat{a}_{th} < a < \hat{a}_{sat} \quad (3)$$

where β_0 and β_1 are regression parameters and ε is the residual (assumed normally distributed) with a zero mean and a standard deviation, σ_ε associated with variability in the imperfect inspection procedure. The probability of detection function, $POD(a)$, for a crack size a , can then be expressed as:

$$POD(a) = P[\hat{a}(a) \geq \hat{a}_{dec}] = \int_{\hat{a}_{dec}}^{\infty} f_{\hat{a}|a}(\hat{a}) d\hat{a} = 1 - F_{\hat{a}|a}(\hat{a}_{dec}) \quad (4)$$

where $f_{\hat{a}|a}(\hat{a})$ and $F_{\hat{a}|a}(\hat{a})$ are the probability density function and the cumulative distribution function, respectively, of the signal value, \hat{a} , for a given crack of size, a . Combining Equations (3) and (4), Berens (1989) suggested the POD function from the signal response method may be estimated as:

$$POD(a) = \Phi \left[\frac{\ln a - [\ln \hat{a}_{dec} - \beta_0] / \beta_1}{\sigma_\varepsilon / \beta_1} \right] \quad (5)$$

where $\Phi(\cdot)$ is the standard normal cumulative distribution function.

In this study, the POD function of each considered NDI technique with respect to the detail of interest reflects its capability. This POD function representing the corresponding NDI technique and other factors such as its cost will affect the optimal inspection procedure selected.

FATIGUE CRACK GROWTH MODEL

Following Paris and Erdogan (1963), Linear Elastic Fracture Mechanics (LEFM) principles have been used in many applications to relate crack growth to the number of stress cycles. An integral form of this relationship is:

$$\int_{a_0}^{a_N} \frac{da}{[F(a)\sqrt{\pi a}]^m} = C \cdot N \cdot S_R^m \quad (6)$$

where a_0 is the initial crack size; a_N is the crack size after N stress cycles; $F(a)$ is a geometry function; m is the fatigue growth exponent; C is a fatigue growth parameter; and S_R is the stress range. If $\Psi(a)$ is defined as the indefinite integral form of the left side term of Equation (6) when the crack reaches a size, a , this equation can be rewritten as:

$$\Psi(a_N) - \Psi(a_0) = C \cdot N \cdot S_R^m \quad (7)$$

Note that, generally, the material properties (C and m) and initial crack size (a_0) are treated as random variables. The crack size, a_N , is then a function of the accumulated number of stress cycles (N) and the stress range (S_R) evaluated for the detail as follows:

$$a_N = \Psi^{-1} \left[\Psi(a_0) + C \cdot N \cdot S_R^m \right] \quad (8)$$

For structural details in a steel bridge, the main source of fatigue loading comes from vehicles, especially trucks. To account for the variable-amplitude stress ranges that result from random truck traffic, the stress range, S_R , in the crack growth model, is usually replaced by an effective stress range, S_{RE} , which represents a weighted effect of stress ranges of all amplitudes that might occur. Schilling et al. (1978) proposed the use of an effective stress range, S_{RE} , for fatigue evaluation:

$$S_{RE} = \left\{ \sum_{i=1}^n \gamma_i \cdot S_{R,i}^3 \right\}^{1/3} \quad (9)$$

where γ_i is the ratio of the number of cycles with i^{th} stress range amplitude, $S_{R,i}$, to the total number of cycles (a total of n ranges are considered). Furthermore, based on the analysis of 51 sets of bridge stress range spectra from six sources including interstate and other routes in semi-rural and metropolitan locations, Schilling et al. (1978) showed that a Rayleigh distribution provides a reasonable model for the stress range spectrum of details in steel bridges. The probability density function for the stress range, S_R , can be expressed as:

$$f_{S_R}(s) = \left(\frac{s}{S_{R0}^2} \right) \cdot \exp \left[-\frac{1}{2} \left(\frac{s}{S_{R0}} \right)^2 \right]; \quad \text{where } S_{R0} = \sqrt{\frac{2}{\pi}} \cdot E[S_R] \quad (10)$$

where $E[S_R]$ is the mean value of S_R , while S_{R0} is a stress value related to $E[S_R]$ as well as to the effective stress range, S_{RE} , which for a Rayleigh distribution analysis is easily expressed in terms of the gamma function, $\Gamma(\cdot)$, as:

$$S_{RE} = \left[E[S_R^m] \right]^{1/m} = \sqrt{2} S_{R0} \cdot \Gamma \left(\frac{m}{2} + 1 \right)^{1/m} \quad (11)$$

Note that the geometry function, $F(a)$, for a specific fatigue detail in a steel bridge may be obtained from available stress intensity manuals or derived using fracture mechanics principles. Also, the number of stress cycles (N) after Y years in service is computed as:

$$N = C_s \cdot (365 \cdot ADTT \cdot Y) \quad (12)$$

where C_s is the number of stress cycles per truck passage and $ADTT$ is the average daily truck traffic crossing the bridge.

Equations (8) and (12) together permit estimation of the crack growth as a function of the number of years, Y , in service. As a special case, when $F(a)$ is taken to be unity, one obtains (see Madsen et al. (1985)):

$$a(Y) = \left[a_0^{(2-m)/2} + \frac{2-m}{2} \cdot \pi^{m/2} \cdot C \cdot S_{RE}^m \cdot (365 \cdot ADTT \cdot C_S \cdot Y) \right]^{2/(2-m)} \quad \text{for } m \neq 2 \quad (13)$$

$$a(Y) = a_0 \cdot \exp\left[\pi \cdot C \cdot S_{RE}^2 \cdot (365 \cdot ADTT \cdot C_S \cdot Y)\right] \quad \text{for } m = 2 \quad (14)$$

According to LEFM principles, fracture results when the stress intensity factor, K , associated with a crack exceeds the fracture toughness, K_c , of the material. In other words, the crack growth relations in Equations (8), (13), and (14) are valid only as long as the crack size remains smaller than the critical crack size, a_{cr} , associated with K_c .

SIMULATION OF CRACK PROPAGATION AND INSPECTION SCENARIOS

Consider a situation where n non-destructive fatigue inspections are performed on a fracture-critical member of a steel bridge at fixed points in time, y_1, y_2, \dots, y_n . In each possible crack growth curve realization, the crack in the detail is assumed to reach its critical crack size at a time, y_{cr} (i.e., $a(y_{cr}) = a_{cr}$). By applying a crack growth model, the size, a_i , of the crack at each inspection time, y_i , can be estimated. By mapping each such crack size, a_i , onto the POD curve for the chosen NDI technique, the probability of detecting the crack size, a_i , denoted as p_i can be estimated. This mapping procedure is shown schematically in Figure 1. The probability of not detecting a crack, P_{nd} , and that of detecting a crack, P_d , before fracture occurs are:

$$P_{nd} = \prod_{i=1}^n (1 - p_i) \quad (15)$$

$$P_d = 1 - P_{nd} = 1 - \prod_{i=1}^n (1 - p_i) \quad (16)$$

where n is the number of inspections before the critical crack size, a_{cr} , is reached. Fixed-interval inspection schedules are considered in this study in order to conform with practical application for bridges. If the inspection interval, y_{int} , and the time to fracture, y_{cr} , are known, the value of n can be obtained without difficulty.

The initial crack size (a_0), material properties (C and m) for the detail, and traffic-related quantities ($ADTT$, C_s , and S_{RE}) are taken as random variables with specified probability distributions. Thus, various crack growth curves arise from Monte Carlo simulations with these random variables. For a specified inspection interval, each crack growth simulation, i , provides two quantities of interest: (i) the probability that a crack is not detected before fracture results, $P_{nd,i}$, and (ii) the number of inspections, n_i , before fracture. Using the results of all the crack growth N_{sim} simulations, the expected probability of not detecting a crack, $E(P_{nd})$, before fracture and the expected number of inspections, $E(n)$, before fracture, can be obtained as:

$$E[P_{nd}] = \frac{1}{N_{sim}} \sum_{i=1}^{N_{sim}} P_{nd,i} \quad (17)$$

$$E[n] = \frac{1}{N_{sim}} \sum_{i=1}^{N_{sim}} n_i \quad (18)$$

By employing a large number of simulations, converged estimates of $E[P_{nd}]$ and $E[n]$ can be obtained. For the given POD curve associated with the selected NDI technique and for the selected inspection schedule, $E[P_{nd}]$ represents the risk of failure to detect an existing crack in a detail before fracture occurs. Also, $E[n]$ represents the expected number of inspections

performed during the fatigue life of the detail (i.e., before fracture occurs). It should be noted that the simulations here do not account for any repair activity.

Because the crack growth curves are simulated randomly by the Monte Carlo method, the time to failure, y_{cr} , in a single simulation may be either longer or shorter than the time, y_1 , when the first inspection is performed. For simulations with detail lives longer than the first inspection time, instead of using Equations (17) and (18), the expected probability of not detecting a crack and the expected number of inspections before fracture may be computed as follows:

$$\begin{aligned}
 E[P_{nd}] &= E[P_{nd} | y_{cr} \geq y_1] \cdot P(y_{cr} \geq y_1) + E[P_{nd} | y_{cr} < y_1] \cdot P(y_{cr} < y_1) \\
 &= \left(\frac{\sum_{i=1}^{N_1} P_{nd,i}}{N_1} \right) \cdot \left(\frac{N_1}{N_{sim}} \right) + \left(\frac{1 \cdot N_2}{N_2} \right) \cdot \left(\frac{N_2}{N_{sim}} \right) \\
 &= \frac{\sum_{i=1}^{N_1} \left[\prod_{j=1}^{n_i} (1 - p_j) \right] + N_2}{N_{sim}}
 \end{aligned} \tag{19}$$

$$\begin{aligned}
 E[n] &= E[n | y_{cr} \geq y_1] \cdot P(y_{cr} \geq y_1) + E[n | y_{cr} < y_1] \cdot P(y_{cr} < y_1) \\
 &= \left(\frac{\sum_{i=1}^{N_1} n_i}{N_1} \right) \cdot \left(\frac{N_1}{N_{sim}} \right) + (0) \cdot \left(\frac{N_2}{N_{sim}} \right) \\
 &= \frac{\sum_{i=1}^{N_1} n_i}{N_{sim}}
 \end{aligned} \tag{20}$$

where N_1 is the number of simulations for which $y_{cr} \geq y_1$; N_2 is the number of simulations for which $y_{cr} < y_1$; N_{sim} ($= N_1 + N_2$) is the total number of simulations; and n_i is the number of inspections in the i^{th} simulation prior to fracture. Note that for simulations where the fatigue life is shorter than the time till the first inspection, the probability of not detecting a crack is 1 since no inspections will have been performed before a_{cr} is reached. A schematic outline of the Monte Carlo simulations and associated computations of $E[P_{nd}]$ and $E[n]$ is presented in Figure 2.

OPTIMAL NDI TECHNIQUE AND SCHEDULE

Practical challenges for bridge inspectors include the need to come up with answers to questions such as “Which NDI technique should I use and how often should I perform the inspections?” In many cases, fracture-critical inspections in steel bridges either follow a fixed two- or one-year interval requirement. However, each bridge has its own unique geometric configuration, design philosophy, and traffic conditions, and even on the same bridge, details may have different expected fatigue performance and can experience quite different levels of stress ranges that will result in different fatigue lives for each detail. Hence, an *ad hoc* fixed inspection interval program may not meet the safety demands for all types of fatigue details on steel bridges. A rational method for selecting a suitable NDI technique and inspection frequency can be useful.

The procedure formulated here seeks to yield a balanced solution that takes into consideration both economy and safety.

Cost Function

In order to represent the problem of selection of a proper NDI technique as an optimization problem, a cost function must be defined that accounts for the consequences of choosing a NDI technique and associated inspection schedule for the detail or member under consideration. Together with the expected number of inspections, $E[n]$, and the expected probability of not detecting a crack, $E[P_{nd}]$, for any NDI technique and inspection schedule, a cost function including the cost of inspections and the expected cost of failure can be assembled.

Cost of Inspections

From the Monte Carlo simulations, $E[n]$ represents the expected number of inspections of the specified detail (prior to failure) for a specified NDI technique and associated inspection schedule. If K_I denotes the cost of a single such inspection, the expected total cost of inspections over the service life, C_I , can be computed as:

$$C_I = K_I \cdot E[n] \quad (21)$$

Cost of Failure

From the Monte Carlo simulations, $E[P_{nd}]$ represents the expected probability of not detecting a crack in the specified detail or member (prior to failure) with the chosen NDI technique and schedule. If, in the simulations, an NDI technique often fails to detect a growing crack in the detail, the associated expected fatigue failure probability will be high. Clearly, $E[P_{nd}]$ provides an indication of the likelihood of fatigue failure of the detail as a result of failure to detect a growing crack with the NDI technique and associated inspection schedule. The risk of fatigue failure for the specified detail can be represented by an estimate of the (expected) cost of failure, C_F . If the detail/member under consideration is fracture-critical, its failure could cause failure of the span where the detail is located or even failure of the entire bridge. Hence, the cost of failure might include the possible cost of rebuilding a span or the entire bridge, as appropriate, as well as costs due to lost use, injuries, fatalities, etc. – not all of these costs are easily and uncontroversially estimated. Nevertheless, all of these potential costs are included in K_F , the cost associated with a failure. The likelihood of such failures is the other term needed to arrive at the expected cost of failure, C_F , which for the specified member or detail may then be defined as:

$$C_F = K_F \cdot E[P_{nd}] \quad (22)$$

Total Cost

Using the definitions of the cost of inspections and failure in Equations (21) and (22) that result from selection of an NDI technique and its associated inspection schedule, the total cost, C_T , may be represented as:

$$C_T = C_I + C_F \quad (23)$$

$$C_T = K_I \cdot E[n] + K_F \cdot E[P_{nd}] \quad (24)$$

Optimization Variables

The POD function corresponding to an NDI technique and the fixed interval, y_{int} , employed in an inspection program are the optimization variables in our optimization problem. The reason for employing a fixed-interval inspection schedule here is to conform to the practical realities of bridge inspections. The POD function for the chosen NDI technique directly affects the value of $E[P_{nd}]$ and the inspection interval, y_{int} , affects both $E[n]$ and $E[P_{nd}]$. Clearly then, the total cost defined in Equation (24) is influenced by the POD function and the inspection interval, y_{int} , in a direct manner. By varying the POD function (or, effectively by choosing a different NDI technique) and the inspection interval, y_{int} , an optimal combination of the two can be found that yields the minimum cost.

Constraints

A target probability level, $P_{nd,\text{max}}$, defined as the maximum allowable probability of not detecting a crack (or the minimum acceptable safety level) for an NDI technique applied on a specified fatigue detail is employed as a constraint in order to exclude combinations of NDI techniques and inspection schedules that might be deemed unsafe because $E[P_{nd}]$ is too high. This constraint can be expressed as:

$$E[P_{nd}] < P_{nd,\text{max}} \quad (25)$$

Additionally, restrictions are placed on the time between inspections so that this inspection interval is neither too large (upper bound, y_{max}) nor too short (lower bound, y_{min}). Such constraints on the inspection interval may be required by local or state transportation agencies. Hence, a second constraint on the inspection interval for the optimization problem is:

$$y_{\text{min}} < y_{\text{int}} < y_{\text{max}} \quad (26)$$

Formulation of the Optimization Problem

In summary, the optimization problem for the selection of an optimal NDI technique and associated inspection schedule may be formulated as follows:

$$\min_{\text{POD}, y_{\text{int}}} C_T = K_I \cdot E[n] + K_F \cdot E[P_{nd}] \quad (27)$$

optimization variables: POD function and inspection interval, y_{int}

subject to: $E[P_{nd}] < P_{nd,\text{max}} ; y_{\text{min}} < y_{\text{int}} < y_{\text{max}}$.

For a given NDI technique (or POD function), an optimum inspection interval, y_{int} , can be found. In addition, by considering alternate NDI techniques, the total cost corresponding to the alternate POD functions can be compared so as to finally yield the optimal choice of NDI technique and associated inspection schedule.

To solve the optimization problem, the Monte Carlo method is employed to estimate the expected probability of not detecting a crack, $E[P_{nd}]$, and the expected number of inspections, $E[n]$, prior to failure for a given NDI technique and an associated inspection schedule by treating the initial crack size (a_0), crack growth parameter (C), and crack growth exponent (m) as random variables. After $E[P_{nd}]$ and $E[n]$ are estimated, the total cost for the given NDI technique and associated schedule can be evaluated. By changing the NDI technique and inspection schedule, repeated computations of total cost are obtained. The optimal choice comes from the NDI technique and schedule that lead to the minimum total cost. A flow chart describing this procedure is presented in Figure 3.

NUMERICAL EXAMPLE

Two full-penetration butt welds in the bottom (tension) flange of a newly built steel box girder bridge are studied in this example for which we seek an optimal NDI technique and inspection schedule. It is assumed that failure of the butt weld detail will result in collapse of the box-girder span. An inherent flaw is assumed to exist in the butt welds of the 1.52 m (60 in.) width (w) bottom flange as shown in Figure 4. The initial flaw size, a_0 , is modeled as a lognormally distributed random variable with a mean value of 0.508 mm (0.02 in.) and a coefficient of variation of 0.5. The critical crack size, a_{cr} , is considered to be constant at 50.8 mm (2 in.) for this example. The fatigue growth parameter, C , is modeled as a lognormal variable with a mean value of 2.18×10^{-13} assuming units of millimeters for crack size and MPa-m^{1/2} for fracture toughness (or, equivalently, 2.05×10^{-10} , assuming units of inches for crack size and ksi-in^{1/2} for fracture toughness) and a coefficient of variation of 0.63. The fatigue growth exponent, m , is modeled as a normally distributed random variable with a mean value of 3.0 and a coefficient of variation of 0.1. The average daily truck traffic, $ADTT$, and the number of stress cycles per truck passage, C_s , for the box girder bridge are taken to be 600 and 1.0, respectively. A Rayleigh distribution with S_{R0} equal to 43.67 MPa (6.334 ksi) is employed to model the stress range spectrum for the bottom flange of the bridge.

Three NDI techniques – ultrasonic inspection (UI), magnetic particle inspection (MI) and penetrant inspection (PI) – are considered here. The POD functions for these three techniques, based on data from flat plate testing results collected by Rummel and Matzkanin (1997), are presented in Figure 5. In practice, the POD functions for these three NDI techniques would need to be obtained from numerous tests of similar butt weld details because POD functions depend on the actual test object (form and material), the anomaly condition, the NDI procedure, and the operator, as was observed by Rummel (1998). The relative costs of the three types of non-destructive inspections and of the cost of failure considered here are: $K_{I,PI} : K_{I,MI} : K_{I,UI} : K_F = 1.0 : 1.2 : 1.5 : 2.0 \times 10^4$. The maximum acceptable probability of not detecting a crack over the service life is taken to be 0.005 – i.e., $E[P_{nd}] < 0.005$ or $P_{nd,max} = 0.005$ – in this example.

Because the initial crack size, a_0 , is relatively small compared to the width of the bottom flange, w (i.e., $a_0/w \approx 3.3 \times 10^{-4}$), the geometry function $F(a)$ is taken to be unity to model the stress intensity factor for the crack. Hence, Equations (13) and (14) can be employed here to predict crack growth rates here. For the detail under consideration, five million Monte Carlo simulations are carried out in order to achieve stable results.

Figure 6 shows costs for various fixed-interval schedules of ultrasonic, magnetic particle, and penetrant inspections, respectively. Each value of y_{int} on the abscissa represents a schedule that employs y_{int} as the inspection interval for the detail under consideration over the service life. Expectedly, one can see a tendency for longer inspections intervals to be associated with lower expected costs of inspections, C_I , but higher expected costs of failure, C_F . On the other hand, schedules with shorter inspection intervals have higher expected costs of inspections, C_I , but lower expected costs of failure, C_F ; the higher inspection costs result due to the increased number of inspections expected with a shorter inspection interval, while the lower expected failure costs result due to the smaller likelihood of failing to detect a crack before fracture occurs. The combined effect of the opposing trends in C_I and C_F with length of inspection interval helps to yield a solution with lowest total cost, $C_{T,min}$, and an optimal inspection schedule, $y_{int,opt}$, for each NDI technique. Before comparing the optimal inspection intervals and costs for the three NDI techniques, the constraint $E[P_{nd}] < 0.005$ needs to be verified first to eliminate any infeasible schedules. As shown in Figure 7, for the ultrasonic inspection, feasible schedules are

only those where the fixed inspection interval is less than or equal to 5 years. Likewise, for magnetic particle and penetrant inspections, the maximum feasible inspection intervals are 4 and 2 years, respectively. After eliminating infeasible schedules, the optimal schedule with the ultrasonic method involves performing inspections every 3 years and leads to a total cost of 63.9 (see Figure 6(a)). For magnetic particle inspections, the optimal schedule involves inspections every 2.5 years and a total cost of 66.1 (see Figure 6(b)). Finally, for penetrant inspections, the optimal schedule involves inspections every 1.5 years and a total cost of 95.4 (see Figure 6(c)). Accounting for the constraint on $E[P_{nd}]$, Figure 8 shows total costs for various fixed-interval inspection schedules with the three NDI techniques. For example, in Figure 8(a), each marker “x” indicates an infeasible schedule that fails to meet the constraint, $E[P_{nd}] < 0.005$. It can be seen that if all three NDI techniques are candidates for inspection of the detail in question, the overall optimal plan would suggest carrying out ultrasonic inspections every 3 years. As summarized in Table 1, even though a single ultrasonic inspection is more expensive than a single magnetic particle or penetrant inspection ($K_{I,PT} : K_{I,MT} : K_{I,UT} : K_F = 1.0 : 1.2 : 1.5$), the less frequent inspections and higher flaw detectability of the UI technique together yield lower total costs than those resulting from use of the other two NDI techniques. Both magnetic particle and penetrant inspections have lower single-inspection costs, but the greater number of inspections and the higher probability of failure to detect a crack (before fracture) resulting from a lower flaw detectability lead to higher total costs than with ultrasonic inspections.

The constraint, $P_{nd,max} = 0.005$ (i.e., $E[P_{nd}] < 0.005$), eliminates some infeasible inspection schedules, typically those with long inspection intervals. A relatively larger number of schedules are eliminated for an NDI technique that has low detectability, such as PI. From Figure 8(a), it can be seen that the optimal schedule for each NDI technique (when $P_{nd,max}$ is 0.005) can be directly identified from the local minima of the three cost curves so that the $P_{nd,max}$ constraint virtually does not affect the optimization solution in this case. However, when a stricter constraint, $P_{nd,max} = 0.001$ (i.e., $E[P_{nd}] < 0.001$), is enforced, a greater number of schedules become infeasible as can be seen in Figure 8(b). The optimal inspection interval for PI, for example, changes from 1.5 years ($C_T = 95.3$) to 1.0 year ($C_T = 104.6$), and for MI, it changes from 2.5 years ($C_T = 66.1$) to 2 years ($C_T = 67.0$). Both these NDI methods demand more frequent inspections to satisfy the stricter $P_{nd,max}$ constraint which, therefore, results in higher total costs. Note that the 3-year inspection interval schedule yielding the minimum total cost ($C_T = 63.9$) for ultrasonic inspections met the original $P_{nd,max} = 0.005$ constraint as well as the stricter $P_{nd,max} = 0.001$ constraint; as a result, the optimal UI schedule is unchanged.

Results from the example above have shown that any *ad hoc* periodic inspection schedule (annual or biennial, for example) without consideration for the quality of inspection may not lead to the optimal schedule for a butt weld detail inspected by any of the three NDI techniques studied here. Besides, if costs are included, useful insights may be gained to guide selection of the optimal inspection strategy using the optimization procedure presented.

CONCLUSIONS

A probabilistic approach for selecting an optimal NDI technique and an associated inspection schedule for fracture-critical members in steel bridges has been presented. The method builds upon LFM principles and detection capabilities of NDI techniques for the fracture-critical member or detail of interest, and then employs Monte Carlo simulations in an optimization problem. Solution of this problem yields the optimal NDI technique and associated inspection schedule for the detail and takes into consideration safety and economy.

Some of the key findings are summarized here:

1. For a given NDI technique, the total cost is controlled by the cost of inspections for schedules with short inspection intervals. This is because the shorter the inspection interval employed, the greater will be the cost of inspections towards total cost. For schedules with longer inspection intervals, the total cost is dominated more by the cost of failure than by inspection costs. Also, the longer the fixed inspection interval, the greater will be the possibility of failure to detect a crack; this leads to higher failure costs. A valley-shaped total cost versus inspection interval curve results. Applying constraints on minimum acceptable safety, some infeasible schedules are eliminated and the optimal schedule for an NDI technique is often found at the bottom of the total cost curve.
2. An NDI technique with a lower crack detectability will generally demand more inspections ($E[n]$) than one with a higher crack detectability to achieve the schedule with minimum total cost. This finding is consistent with practical experience where more inspections are needed for an NDI technique with a low crack detectability.
3. Ideally, the optimal inspection schedule for a fracture-critical member should consider both cost and quality of the NDI technique. If POD data are available for candidate NDI techniques, the procedure presented here can include consideration for cost and safety to yield an optimal inspection schedule (instead of any *ad hoc* periodic inspection schedule). Optimization results are directly affected by the NDI detectabilities (i.e., POD functions), the constraint on the largest permitted expected probability of not detecting a crack, $E[P_{nd}]$, and the relative costs of inspection and failure.
4. An NDI technique with higher detectability for cracks will tend to yield lower $E[P_{nd}]$ values. This leads to lower costs of failure in the total cost. However, an NDI technique with a higher crack detectability is usually more expensive and will involve higher inspection costs.
5. Regarding the effect of the $P_{nd,max}$ constraint, it is found that upon raising the required safety level for a detail, schedules with longer time between inspections become unacceptable because they can cause higher $E[P_{nd}]$ values than the prescribed value of $P_{nd,max}$. Upon decreasing the $P_{nd,max}$ value, the optimal schedule adjusts to a shorter inspection interval. This trend is in agreement with experience where higher safety levels generally demand more frequent inspections (i.e., a shorter inspection interval).

ACKNOWLEDGEMENTS

The authors acknowledge financial support through a research grant awarded by the Texas Department of Transportation as part of the project, Inspection Guidelines for Fracture Critical Steel Trapezoidal Girders.

REFERENCES

- (1) Hartle, R. A., Amrhein, W. J., Wilson III, K. E., Bauhman, D. R. and Tkacs, J. J. (1995). "Bridge Inspector's Training Manual 90." *FHWA-PD-91-015*, Federal Highway Administration, Washington, D.C.
- (2) Sorensen, J. D., Faber, M. H., Rackwitz, R. and Thoft-Christensen, P. (1991). "Modelling in Optimal Inspection and Repair." *Proceedings of the 10th International Conference on Offshore Mechanics and Arctic Engineering*, ASME, Vol. 2, Stavanger Norway, pp. 281-288.

- 1
- 2
- 3
- 4 (3) Cramer, E. H. and Friis-Hansen, P. (1992). "Reliability Based Optimization of Multi-
- 5 Component Welded Structures." *Proceedings of the 11th International Conference on*
- 6 *Offshore Mechanics and Arctic Engineering*, ASME, Vol. 2, Calgary Canada, pp. 265-271.
- 7 (4) Berens, A. P. and Hovey, P. W. (1981). "Evaluation of NDE Reliability Characterization."
- 8 AFWAL-TR-81-4160, Vol. 1, Air Force Wright-Aeronautical Laboratory.
- 9 (5) Johnson, R. A. (2000). *Miller and Freund's Probability and Statistics for Engineers*, 6th
- 10 Edition, Prentice-Hall Inc., New Jersey.
- 11 (6) Berens, A. P. (1989). NDE Reliability Analysis. In: *Metals Handbook*, Vol. 17. 9th ed.
- 12 ASM International, pp. 689-701.
- 13 (7) Paris, P. C. and Erdogan, F. (1963). "A Critical Analysis of Crack Propagation Laws."
- 14 *Journal of Basic Engineering*, ASME, Vol. 85, pp. 528-534.
- 15 (8) Schilling, C. G., Klippstein, K. H., Barsom, J. M., and Blake G. T. (1978). "Fatigue of
- 16 Welded Steel Bridge Members under Variable-Amplitude Loadings." *National Cooperative*
- 17 *Highway Research Program Report 188*, Transportation Research Board, Washington,
- 18 D.C.
- 19 (9) Madsen, H. O., Krenk, S. and Lind, N. C. (1985). *Methods of Structural Safety*, Prentice-
- 20 Hall Inc., New Jersey.
- 21 (10) Rummel, W. D. and Matzkanin, G. A. (1997). *Nondestructive Evaluation Capabilities Data*
- 22 *Book*, Nondestructive Testing Information Analysis Center, Austin, Texas.
- 23 (11) Rummel, W. D. (1998). "Probability of Detection as a Quantitative Measure of
- 24 Nondestructive Testing End-to-End Process Capabilities." *Materials Evaluation*, Vol. 56,
- 25 No. 1, pp. 29-35.
- 26
- 27
- 28
- 29
- 30
- 31
- 32
- 33
- 34
- 35
- 36
- 37
- 38
- 39
- 40
- 41
- 42
- 43
- 44
- 45
- 46
- 47
- 48
- 49
- 50
- 51
- 52

**TABLE 1 Optimization Results for the UI, MI and PI Techniques
with the Constraint, $P_{nd,max} = 0.005$.**

NDI Technique	$E[n]$	$E[P_{nd}]$	$y_{int,opt}$ (years)	$C_{T,min}$
Ultrasonic	31.2	8.26×10^{-4}	3.0	63.9
Magnetic Particle	38.0	1.02×10^{-3}	2.5	66.1
Penetrant	63.6	1.59×10^{-3}	1.5	95.3

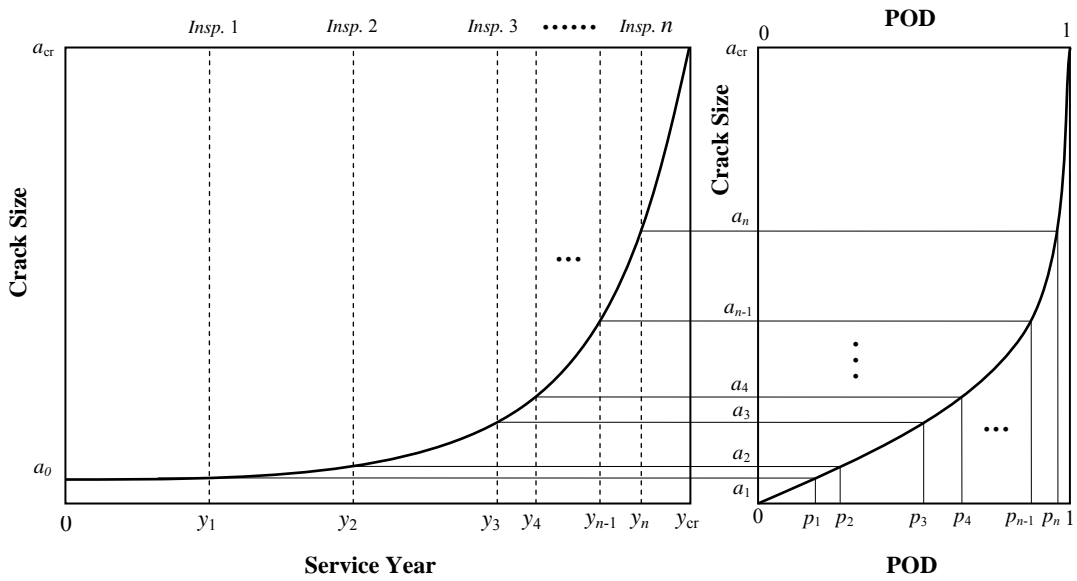


FIGURE 1 Mapping of Crack Size with Probability of Detection and Time in Service.

1
2
3
4
5
6
7
8
9
10
11
12
13
14
15
16
17
18
19
20
21
22
23
24
25
26
27
28
29
30
31
32
33
34
35
36
37
38
39
40
41
42
43
44
45
46
47
48
49
50
51
52

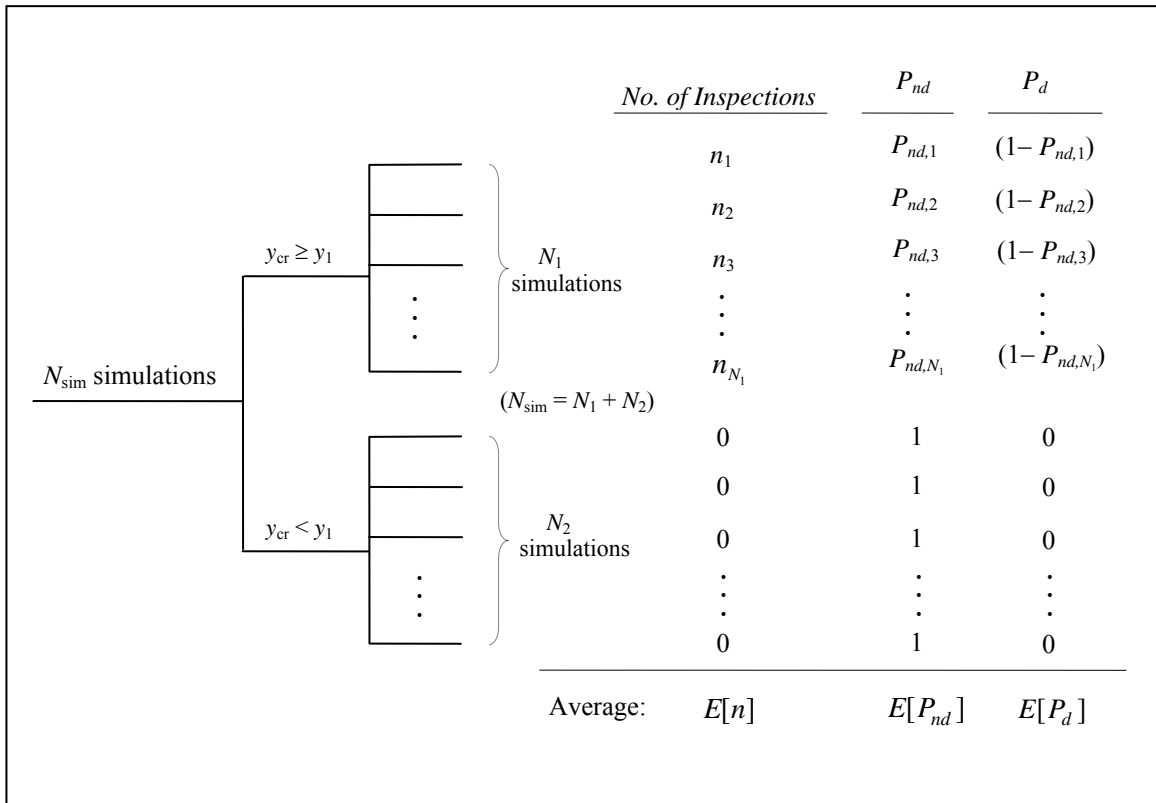


FIGURE 2 Monte Carlo Simulation Scenarios and Associated Computations.

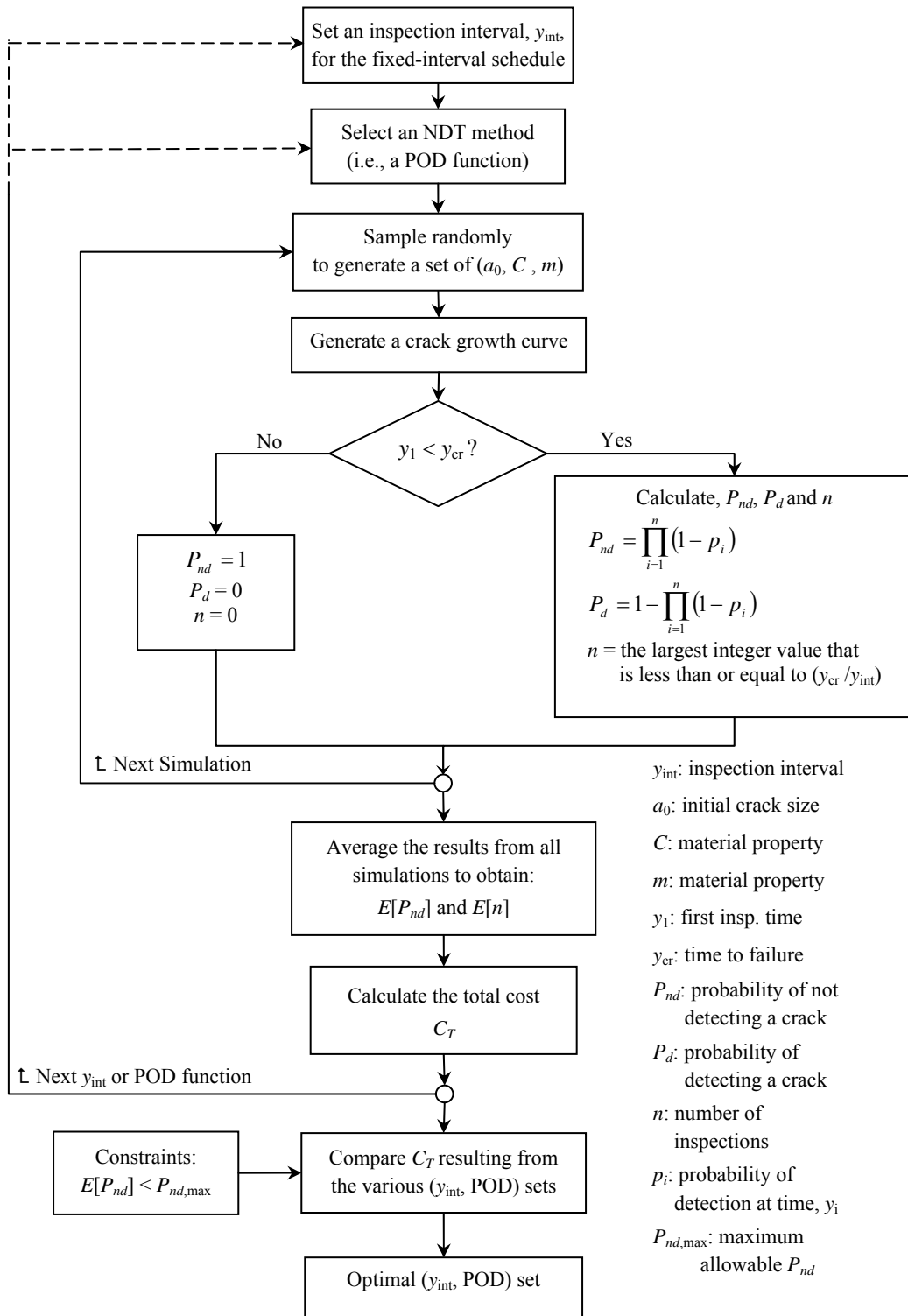


FIGURE 3 Flow Chart of the Optimization Procedure.

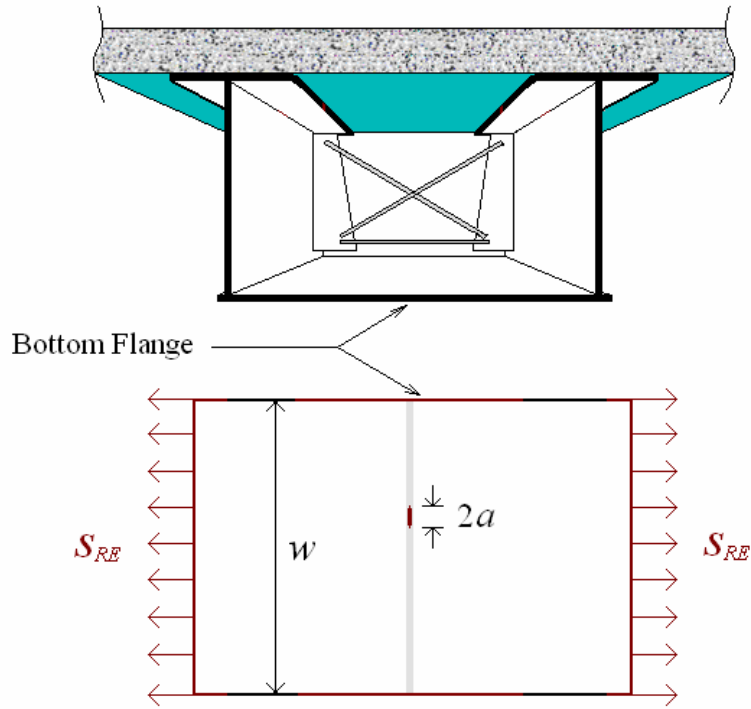


FIGURE 4 Detail in a Fracture-Critical Member of the Box Girder Bridge.

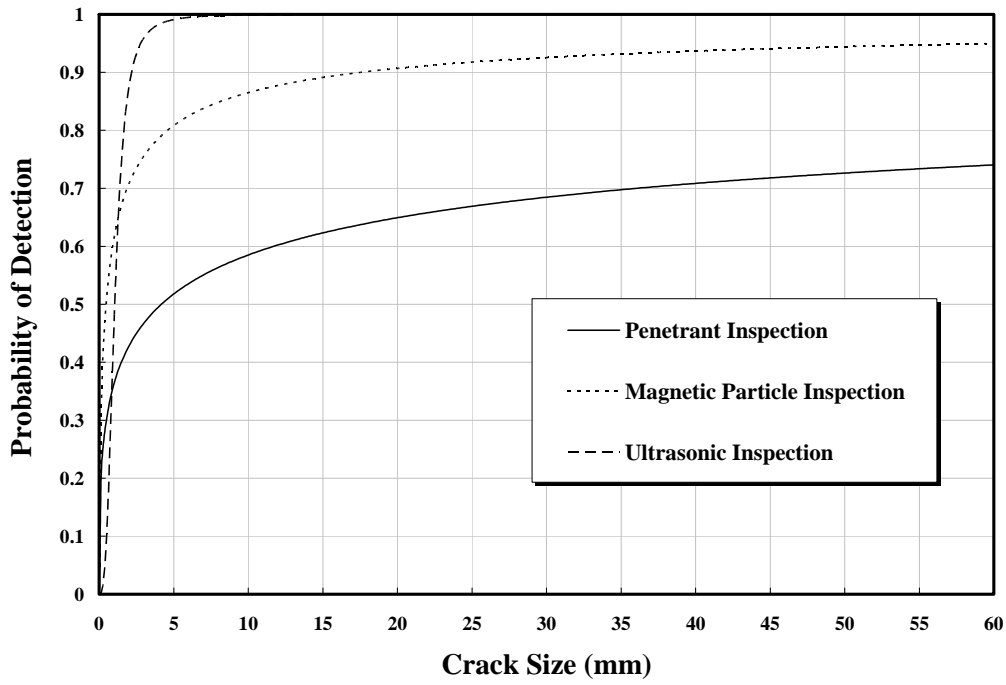
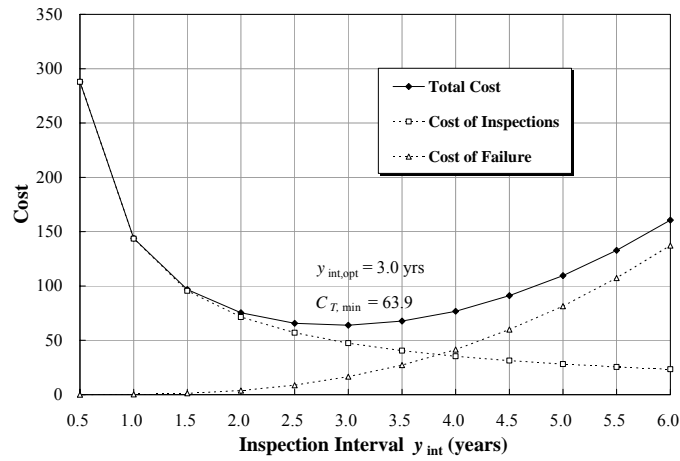
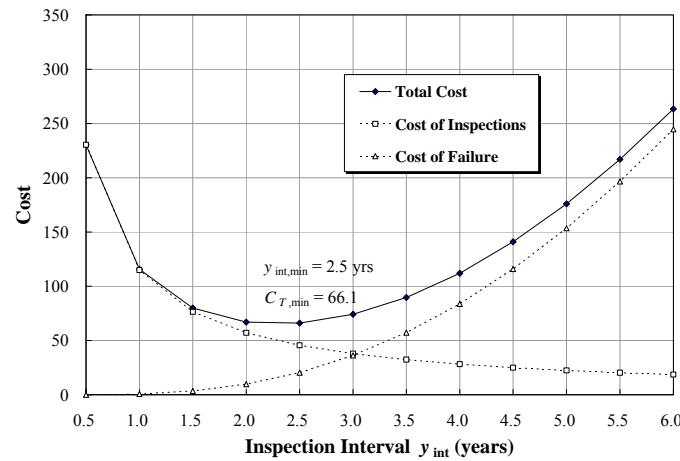


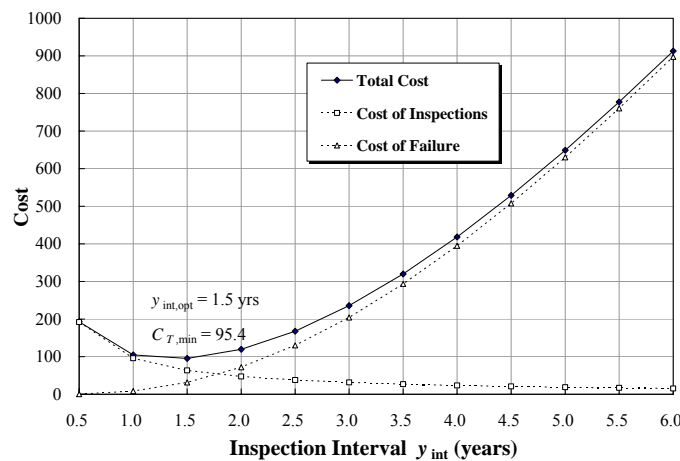
FIGURE 5 Probability of Detection (POD) Curves for Penetrant, Magnetic Particle, and Ultrasonic Inspections.



(a)



(b)



(c)

FIGURE 6 Costs for Various Fixed-Interval Schedules for $K_{L,UI} : K_F = 1.5 : 2 \times 10^4$ with (a) Ultrasonic, (b) Magnetic Particle, and (c) Penetrant Inspections.

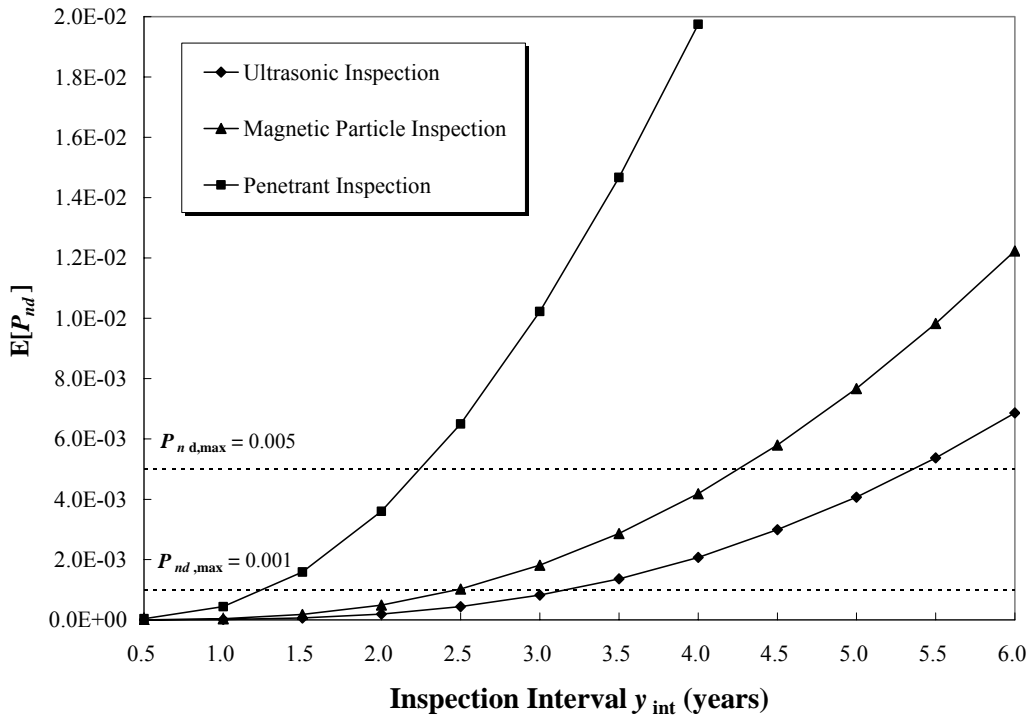
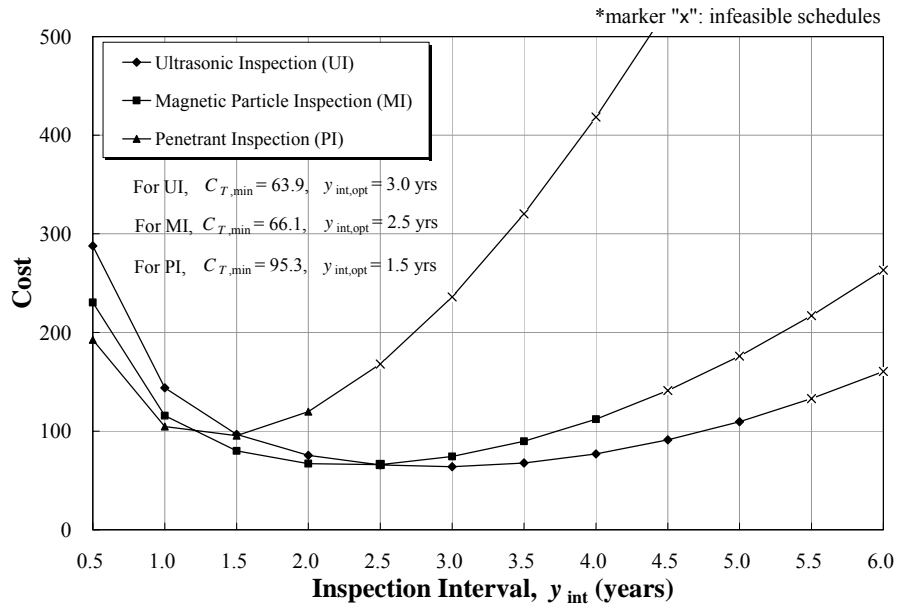
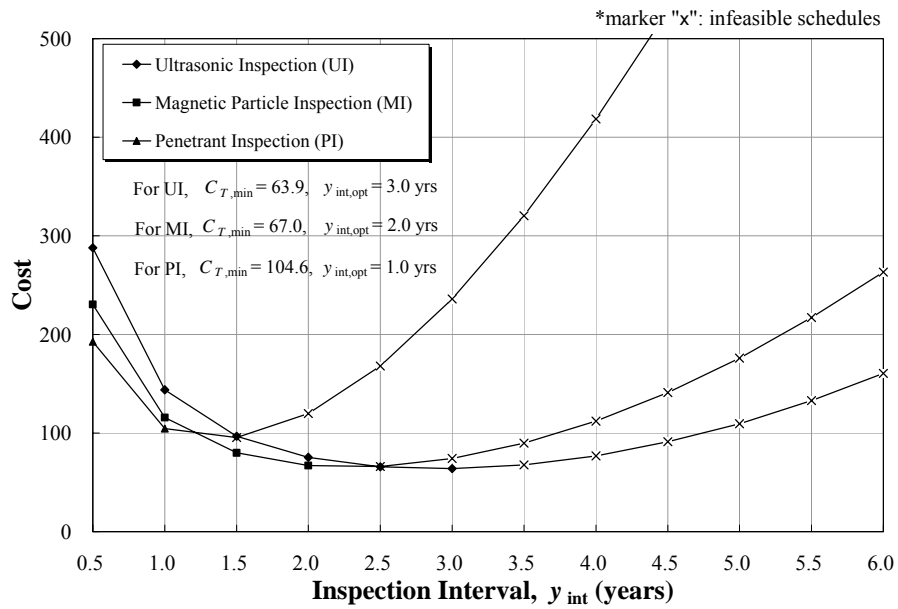


FIGURE 7 Expected Probabilities of Failure to Detect a Growing Crack before Fracture, $E[P_{nd}]$, for the UI, MI and PI Techniques compared with the Maximum Acceptable Probability of Non-Detection, $P_{nd,max}$.



(a)



(b)

FIGURE 8 Cost Comparison of UI, MI and PI in Various Fixed-Interval Schedules for $K_{I,PI} : K_{I,MI} : K_{I,UI} : K_F = 1.0 : 1.2 : 1.5 : 2 \times 10^4$ showing Infeasible Schedules when (a) $P_{nd \max} = 0.005$ and (b) $P_{nd \max} = 0.001$.